Few-Body Systems 40, 237–252 (2007)
DOI 10.1007/s00601-007-0175-5
Printed in The Netherlands

Few-Body Systems

Temperature Effects on Electron Correlations in Two Coupled Quantum Dots

M. Leino* and T. T. Rantala**

Institute of Physics, Tampere University of Technology, P.O. Box 692,
FI-33101 Tampere, Finland

Received February 9, 2007; accepted April 19, 2007
Published online May 25, 2007;

Abstract. The path-integral Monte Carlo simulation method is used to examine one and two electrons in a system of two coupled disc-like quantum dots (QD) in a zero magnetic field. With this approach we are able to evaluate the one-electron distributions and two-electron correlation functions, and finite temperature effects on both. Increase of temperature broadens the distributions as expected, the effect being smaller for correlated electrons than for single ones. The simulated one- and two-particle distributions of a single and two coupled quantum dots are also compared to those from other theoretical methods. For the one-particle distributions we find a good agreement with those from the DFT approach. The effect of the third dimension or the thickness of the almost two-dimensional disc-like QDs is small for the one-particle distributions, but it is clearly seen in the electron-electron correlation or the two-particle distribution function at low temperatures. The mutual Coulomb energy of the two electrons is found to be temperature-independent, and also, independent of the correlation effects on the dynamics. Computational capacity is found to become the limiting factor in simulations with increasing accuracy or increasing number of particles, and in case of fermions in particular. This and other aspects of PIMC and its capability for this type of calculations are also discussed.

1 Introduction

Special features of the electronic structure of small quantum-confined systems has drawn much attention during the last years. This is largely a consequence of developments in semiconductor technology, where it has become possible to devise

* *E-mail address*: Markku.Leino@tut.fi
** *E-mail address*: Tapio.Rantala@tut.fi

nanometer scale confinement in one, two or three dimensions [1–4]. Confinement in three dimensions leads to smallest systems, quantum dots (QD), containing possibly only a few charge carriers. The electronic structure of a few-electron system is subject to strong many-body effects, and therefore makes a distinctive challenge to the conventional density-functional (DFT) approach, the standard formalism of theoretical solid-state and semiconductor physics. Emanation of the finite-temperature effects is another challenge beyond the standard approaches.

Quantum Monte Carlo methods offer a possibility to treat the many-body correlations exactly with an accuracy depending on the available computing power only. On the other hand, the path-integral formalism of quantum statistics allows one to include finite temperature using a description with mixed states. The combination of these two, the path-integral Monte Carlo (PIMC) approach, permits inspection of the interplay of both, i.e., the temperature effects in many-body correlations. Earlier, we have used this approach to study two electrons in a strongly confining model QD [5]. Mixed state densities, energies and pair correlation functions and their temperature dependencies were evaluated. We also showed how pure states can be searched using the density matrices from several different temperatures. In this paper we report a PIMC study of a system consisting of two coupled QDs, a system which has also been studied experimentally [4].

As QDs are sometimes called artificial atoms, the coupled QDs have been considered as molecules with delocalized electronic states. The electronic properties of single and coupled QDs created with layer-by-layer semiconductor growth can be selected with some freedom by tailoring the shape of a lateral confining potential and the range of vertical confinement [4]. The grown QDs are usually confined vertically in nanometer scale, but laterally in a one to two orders of magnitude larger range. Such dots can be approximately treated as two-dimensional disk-like electronic systems [6]. The ‘‘dimensionality effect’’ or separability of such systems to one- and two-dimensional subsystems is still considered to be an open question. Thus, the effect of a small but finite vertical extension on the QD structure is worth studying [4, 6].

We restrict our present study to systems with one or two electrons, only. By separating the vertical and lateral electronic wave functions the single electron case can be treated analytically. It then serves as a reference case to study the dimensionality effect or separability in the two-electron system. On the other hand, the two-electron system is also the simplest system to study the correlations and its dependence on temperature. With the two-electron system we do not involve the exchange interaction by restricting ourselves to two ‘‘spinless electrons’’ only.

The two-electron system is one of the simplest non-trivial quantum mechanical systems. Nevertheless, some analytical results exist for two electrons in a symmetrical enough quantum dot. Taut [7] reduced the problem of solving a six-dimensional partial differential equation to finding the real roots of a polynomial, and thus gave analytic solutions to particular oscillator frequencies of two interacting electrons in an external harmonic oscillator potential. Dineykhan and Nazmitdinov [8] found analytical expressions for the ground-state energy for 2D and 3D harmonic oscillators in an external magnetic field.

In addition to analytical results, there are a number of numerical results for (harmonic) two-electron quantum dots. A numerically exact calculation for the

energy spectra of two electrons in a finite-height cylindrical quantum dot by a coupled-channel method is presented in details by Lin and Jiang [9]. Harju et al. [10] studied the ground state of parabolically confined electrons in a quantum dot by both direct numerical diagonalization and variational quantum Monte Carlo methods. In an older paper Harju et al. [11] applied the quantum Monte Carlo technique to a two-electron quantum dot. Merkt, Huser, and Wagner [12] have calculated the discrete energy spectra for two electrons in a two-dimensional harmonic well in the effective-mass approximation as a function of the dot size and the strength of a magnetic field directed perpendicular to the dot plane using the first-order perturbation theory. Furthermore, the states of two-electron paired quantum-well quantum dots [13, 14] were calculated with diagonalization and the variational principle. A spin-exchange coupling J between two electrons in tunnel-coupled quantum dots is determined by Burkard et al. [15] by the Heitler-London and Hund-Mulliken techniques.

The ground-state behavior of a 3D quantum dot with square well in z-dimension is studied by Lee et al. [16]. The coupled quantum dots are studied by Partoens and Peeters [17] and Pi et al. [4] within the spin-density functional theory. The latter one serves as reference approach to ours as the studied system is similar. Wensauer et al. [18] present ground-state calculations for laterally coupled quantum dots containing two, four and eight electrons using the spin-density functional theory. Pi et al. [19] investigate computationally and experimentally the dissociation of few-electron circular vertical-semiconductor double-quantum-dot artificial molecules at 0 K as a function of the interdot distance. Excited-state properties of vertically coupled double quantum dots are studied by Imamura et al. [20] by exact diagonalization. Tanaka and Akera [21] calculated the exact many-body eigenstates in a quantum dot formed in double-barrier heterostructures, and they studied coherent transport through the states.

More complicated quantum dots have been studied by many methods: perturbation theory [22], numerical diagonalization [23], density-functional theory [24, 25], unrestricted Hartree-Fock [26], diffusion Monte Carlo [27] and path-integral Monte Carlo [3, 28–31] methods. In these studies the electronic structure, addition spectra, electronic states, Fermi liquid and Wigner molecule behaviour, ground and excited state energies, shell effects, electron correlations and low-energy states were examined.

The next section briefly presents the PIMC method and details of our simulation procedure. In Sect. 3 we describe the two-coupled-dots system that we are interested in, with the relevant analytical one-particle distributions and energetics. The two last sections report the simulation results and our conclusions for the two-electron system.

2 Method

2.1 Path-Integral Monte Carlo Method

All stationary properties of a quantum many-body system with Hamiltonian $\widehat{H}$ in thermal equilibrium are obtained from the density matrix [32] $\hat{\rho} = \exp(-\beta\widehat{H})$ as expectation values $\langle\widehat{A}\rangle = Z^{-1}\,\mathrm{Tr}(\hat{\rho}\widehat{A})$, where $\beta \equiv (k_{\mathrm{B}}T)^{-1}$ is the inverse tem-

perature, $\widehat{A}$ is the operator of the property in question and $Z = \mathrm{Tr}(\hat{\rho})$ is the partition function.

In the position representation the density matrix $\hat{\rho}$ reads as

$$\rho(\boldsymbol{R}, \boldsymbol{R}'; \beta) = \langle \boldsymbol{R} | \exp(-\beta \widehat{H}) | \boldsymbol{R}' \rangle, \tag{1}$$

where $\boldsymbol{R} = (\boldsymbol{r}_1, \boldsymbol{r}_2, \ldots, \boldsymbol{r}_N)$ are the coordinates of the N particles. Thus, the one-particle distribution is

$$\begin{aligned} \rho(\boldsymbol{r}) &= \int \rho(\boldsymbol{R}, \boldsymbol{R}; \beta)\, d\boldsymbol{r}_2\, d\boldsymbol{r}_3 \cdots d\boldsymbol{r}_N \big|_{\boldsymbol{r}_1 = \boldsymbol{r}} \\ &= \int \delta(\boldsymbol{r} - \boldsymbol{r}_1) \rho(\boldsymbol{R}, \boldsymbol{R}; \beta)\, d\boldsymbol{R} \end{aligned} \tag{2}$$

and the simple 1D pair-correlation function for two particles is

$$g(r) = \int \delta(r - |\boldsymbol{r}_1 - \boldsymbol{r}_2|) \rho(\boldsymbol{R}, \boldsymbol{R}; \beta)\, d\boldsymbol{R}, \tag{3}$$

assuming normalization of the density by

$$\int \rho(\boldsymbol{R}, \boldsymbol{R}; \beta)\ d\boldsymbol{R} = 1. \tag{4}$$

The path-integral representation of the density matrix discretized in the primitive approximation [33] is a multidimensional integral [34, 35], which turns out to be a partition function of one specific classical many-particle canonical ensemble or NVT-system with

$$Z = N_Z \int \exp\left[-\beta \sum_{n=1}^{M} (K_n + U_n) \right] d\boldsymbol{r}_1 \cdots d\boldsymbol{r}_M, \tag{5}$$

where the normalization constant $N_Z = (mM/(2\pi\hbar^2\beta))^{dN/2}$ and internal and external energies of the system are described by K_n and U_n, respectively. They are written as

$$K_n = \frac{mM}{2\hbar^2\beta^2} (\boldsymbol{r}_{n-1} - \boldsymbol{r}_n)^2, \tag{6}$$

$$U_n = \frac{1}{2M} (V(\boldsymbol{r}_{n-1}) + V(\boldsymbol{r}_n)), \tag{7}$$

and $V(\boldsymbol{r})$ is a local external potential, and we require periodic boundary conditions in imaginary time τ, i.e., all paths have to be closed, and thus, $\boldsymbol{r}_0 = \boldsymbol{r}_M$. The primitive approximation is exact at the limit $\tau = \beta/M \to 0$, and thus it will converge to the correct description, given small enough τ. Furthermore, it ''contains all the physics'' and it is simple and well defined [33].

This specific classical system consists of N closed chains or ''polymers'' or ''necklaces'' of M knots or ''beads'' with a certain special description of interactions among the N particles and between the external potential. The Trotter number M is the degree of discretization. This is the famous mapping from a quantum system to a classical system [33].

The quantum kinetic energy part corresponds to a classical spring potential connecting neighbouring beads representing the same particle. The interbead

potential (spring constant) depends on both M and $\beta = 1/k_{\mathrm{B}}T$. It is easier to obtain a good approximation to the high-temperature density matrix with respect to M, since the high-temperature behavior is more classical-like [36]. The lower the temperature, the more beads on the necklace are needed for the proper quantum description. We will demonstrate this below.

In summary, the description of a finite-temperature quantum statistical system is reduced to that of one specific classical NVT-system. For simulation of this there is the powerful Metropolis Monte Carlo (MMC) algorithm [37]. Thus, PIMC is a combined path-integral formalism and MMC, that has shown to be a powerful computational technique, capable of simulating boson systems exactly and fermions accurately [36]. Furthermore, with this technique all the approximations are controllable.

It is straightforward to calculate scalar operators, such as density, the potential energy, and the pair correlation functions as they are simply averages over the paths [33]. Use can be made of the symmetry in imaginary time, since all time slices are equivalent. Thus, the average density is

$$\rho(\boldsymbol{r}) = N_\rho \sum_{n,i,t} \langle \delta(\boldsymbol{r} - \boldsymbol{r}_{nit}) \rangle \tag{8}$$

where n refers to different beads of particles, i and t to MMC steps. This can be evaluated directly during the stationary simulation process. Similarly, data for the 3D pair correlation function

$$g(\boldsymbol{r}) = N_g \sum_{n,i\neq j,t} \langle \delta(\boldsymbol{r} - (\boldsymbol{r}_{nit} - \boldsymbol{r}_{njt}) \rangle \tag{9}$$

can be collected from the MMC path.

The nondiagonal properties in coordinate basis, such as the energy, the free energy, and the momentum distribution, are not so straightforward to calculate. The thermodynamic estimator of the energy is obtained by differentiating the partition function with respect to the inverse temperature [33]

$$E_T = -\frac{1}{Z}\frac{dZ}{d\beta} = M\langle dN/(2\beta) - K_n + V_n/M \rangle. \tag{10}$$

So, the path-integral Monte Carlo simulation method is a formally exact finite-temperature approach, where the only limiting factor is the computational capacity needed for evaluation of the density matrix $\rho(\boldsymbol{R}, \boldsymbol{R}'; \beta)$ with large enough Trotter number M.

2.2 Simulation Procedure and Parameters

We run Metropolis Monte Carlo in its standard form, only searching for the effective algorithm for random sampling of the configuration space.

In the simplest choice for the transition probability, *the classic rule*, a single particle at a single time slice is displaced uniformly inside a cube of side length Δ, adjusted to achieve 50% acceptance rate. This is inefficient at very large particle numbers: Interactions prevent sizeable displacements of a single particle [38]. As

the main issue is whether the configuration space is explored thoroughly in a reasonable amount of computing time obeying the principle of detailed balance, we do the following.

We include many types of moves, which makes the algorithm more robust. We separate the steps in the *xy*-plane and *z*-direction. We have two types of steps, one for a randomly selected bead in one random necklace and another for the centre of mass of the necklace. We use the classic rule such that the acceptance frequency of each move is about the same. The step lengths vary from 0.5 to 9 nm in both the *z*-direction and the *xy*-plane for one bead and for the centre of mass from 0.05 to 3 nm in the *z*-direction and from 10 to 50 nm in the *xy*-plane.

We choose the Trotter numbers in powers of 2. Using small Trotter numbers, the stationary state can be achieved more easily. Therefore, we found it useful to take the initial configuration for the case $M = 2^n$ from the $M = 2^{n-1}$ case by doubling the number of beads: inserting one more between the existing ones. The above choice of moves prevents us using too large Trotter numbers (larger than 2^{11}) because the configuration space should be explored thoroughly in a reasonable amount of computer time.

To check out the choice of parameters and the numerical scheme we have carried out extensive and systematic tests.

3 Two Coupled Quantum Dots

3.1 Structure Parameters

The system of two vertically coupled QDs is taken from Pi et al. [4]. They have considered it experimentally and realized by semiconductor technology as a layered circular mesa with two axially symmetric GaAs QDs with electrodes to control the number of trapped electrons. Thus, the vertical confining potential consists of two quantum wells of depth 300 meV and width of $W = 12$ nm and a barrier in between of width $b = 2.4$ nm. The potential profile is shown in Figs. 1 and 2, below.

In this two-electron problem the exact Hamiltonian reduces to the centre of mass (CM) and the relative motion [6]. The CM solutions are known analytically, but the relative motion must be determined numerically.

The two-dimensional lateral confinement is approximated by a harmonic potential assuming circular symmetry and ''strength'' $\hbar\omega = 5$ meV. Thus, the system consists of two disc-like QDs axially on top of each other, with the disc diameter an order of magnitude larger than the disc thickness.

Assuming GaAs material parameters throughout the structure, we use the electron effective mass $m^\star = 0.067 \times$ free electron mass and the dielectric constant $\epsilon = 12.4$ everywhere.

3.2 Analytical Distribution Functions

The three-dimensional wavefunction and distributions of a single electron are separable to three one-dimensional contributions in this geometry. In the present case, however, we find it more representative to project out the one-dimensional vertical

and the two-dimensional lateral contributions. Thus, we define the projected one-particle densities

$$\rho_z(z) = \int \rho(\boldsymbol{r})\, dx\, dy \tag{11}$$

and

$$\rho_{xy}(r_{xy}) = \int \rho(\boldsymbol{r})\, dz, \tag{12}$$

where $r^2 = r_{xy}^2 + z^2 = x^2 + y^2 + z^2$. Similarly we define for the pair correlation functions

$$g_z(z) = \int \delta(z - |z_1 - z_2|)\rho(\boldsymbol{R}, \boldsymbol{R}; \beta)\, d\boldsymbol{R} \tag{13}$$

and

$$g_{xy}(r_{xy}) = \int \delta(r_{xy} - |r_{1xy} - r_{2xy}|)\rho(\boldsymbol{R}, \boldsymbol{R}; \beta)\ d\boldsymbol{R}. \tag{14}$$

These can be readily evaluated from the analytical one-electron distributions for a single electron (or two noninteracting electrons) in our coupled QD model. The vertical unnormalized wave function for the symmetrical double quantum well is [39]

$$u(z) = \begin{cases} \cosh kz \quad \text{or} \quad \sinh kz, & \text{for} \quad 0 < z < b/2, \\ A \sin qz + B \cos qz, & \text{for} \quad b/2 < z < b/2 + W, \\ Ce^{-kz}, & \text{for} \quad z > b/2 + W, \end{cases} \tag{15}$$

where $k^2 = |E_z|/\lambda$, $q^2 = (V - |E_z|)/\lambda$, $\lambda = \hbar^2/2m^\star$, E_z is the (quantized) eigenenergy and the constants A, B, and C are chosen to make the wave function and its derivative continuous. The functions $\cosh(kz)$ and $\sinh(kz)$ are the even and odd parity solutions, respectively, implying an obvious behavior of $u(z)$ at $z < 0$, not written in Eq. (15), explicitly.

The finite-temperature density matrix can be written now as

$$\rho(z, z'; \beta) = N(\beta) \sum_i u_i^*(z) u_i(z') \exp[-\beta E_{iz}], \tag{16}$$

where at low temperatures we can restrict to the sum over a finite number of lowest quantum states and $N(\beta) = \left\{\sum_i \exp[-\beta E_{iz}]\right\}^{-1}$. Similarly the energy expectation value is obtained from

$$\langle E_z \rangle = \sum_i E_{iz} \exp[-\beta E_{iz}], \tag{17}$$

which should be evaluated numerically as the eigenenergies are solved from implicit equations.

Note that there is only a finite number of bound states in the potential well of finite depth V, over which the summing is carried out. Omission of the continuum states introduces an error, which is, however, negligible at such low temperatures considered here.

In the horizontal plane the case is a simple two-dimensional harmonic oscillator, found in good text books of quantum mechanics. The two-dimensional one-electron finite-temperature electron distribution is

$$\rho_{xy}(\boldsymbol{r}_{xy}, \boldsymbol{r}'_{xy}) \propto \exp\left[\frac{-m\omega}{2\hbar \sinh(\hbar\omega\beta)} \times ((\boldsymbol{r}_{xy}^2 + \boldsymbol{r}_{xy}'^2)\cosh\hbar\omega\beta - 2\boldsymbol{r}'_{xy} \cdot \boldsymbol{r}_{xy})\right] \tag{18}$$

and the energetics can be summed up, giving

$$\langle E_{xy}\rangle = 2\frac{\hbar\omega}{2}\coth\frac{\hbar\omega\beta}{2}. \tag{19}$$

While the level spacing in the vertical quantum problem is about 50 meV, in the horizontal harmonic oscillator it is 5 meV with the degeneracy increasing linearly

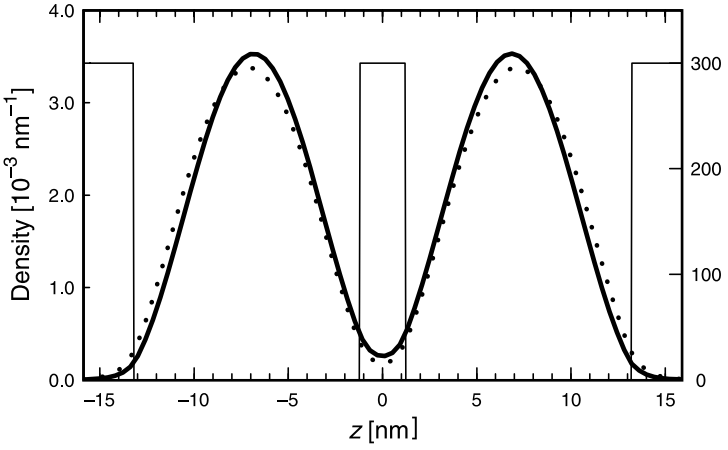

Fig. 1. Analytical vertical (z) one-particle distribution functions at different temperatures in the confining potential of 300 meV. The probability distributions $\rho(z)$ are in arbitrary units but normalized to the same constant. The shown distributions are 10 K (solid) and 300 K (dotted)

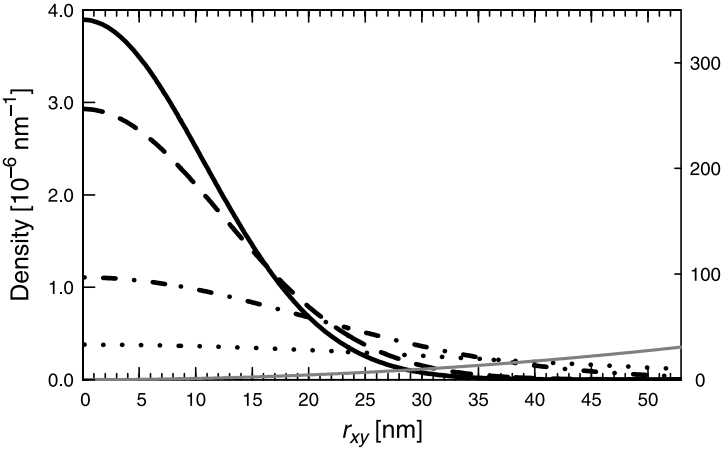

Fig. 2. Analytical horizontal (xy) one-particle distribution functions at different temperatures and the confining potential with $\hbar\omega = 5$ meV (~ 30 meV at 50 nm). The two-dimensional integrals (with a weight $4\pi r^2$) of shown distributions are normalized to the same constant. The distributions are from 10 K (solid), 30 K (dashed), 100 K (dash-dotted), and 300 K (dotted)

in energy. The separable energy contributions from the z confinement and xy harmonic potential simply add up.

The vertical and horizontal confining potentials and distributions are shown in Figs. 1 and 2, respectively. The confinement is seen to be one to two orders of magnitudes stronger in the vertical direction, resulting in essential differences in the temperature response of the one-particle density.

In Fig. 1 it is seen that only at 300 K a small shift of the density away from the centre barrier takes place, resulting in a decrease of tunneling there. This is probably a contribution from the continuum states. Fig. 2, on the contrary, shows the strong temperature broadening, as expected.

Like the energies, the densities of separable dimension simply ''add up'', too. From these one-particle densities we have calculated the pair correlation functions of the two noninteracting electrons, to be used as a reference in search of the two-electron correlation effects, later. The two-noninteracting-electron pair correlation function is a simple convolution-like distribution.

4 Simulation Results

4.1 Single Electron Distributions and Energies

Simulations with large enough Trotter numbers accurately reproduce the analytical one-particle distributions of the single-electron system (or two noninteracting electrons) shown in Figs. 1 and 2 both as vertical (z) and lateral (xy) projections of the three-dimensional distribution, respectively. Due to the limited computing capacity we were able to verify this at higher temperatures, $T \geq 10$ K, only.

The analytical temperature-dependent energies are easily obtained from Eqs. (17) and (19). The 2D harmonic oscillator energy raises from the zero-Kelvin quantum limit 5 meV to about 18 and 52 meV at 100 and 300 K, respectively. The corresponding energies for the 1D ''vertical'' double QD are about 24, 25, and 30 meV, in the same order. Whereas the contributions from the kinetic and potential energies are equal in case of the harmonic oscillator, the 1D ''vertical potential energy'' is about 6 meV at all temperatures. The sum of the 1D and 2D contributions yields the total energies 29, 43, and 82 meV, for the zero-Kelvin quantum limit, 100 and 300 K, respectively.

At lower temperatures higher Trotter numbers are required to reach the quantum statistical limit. Below this limit the correct quantum statistical behavior is not found, but classical-like features emerge. For example, discontinuous distributions at potential discontinuities are seen. On the other hand, this can be used to demonstrate the classical-to-quantum transition, see Fig. 3, where for the lowest temperature $T = 3$ K the Trotter number $M = 2048$ is clearly too small, or correspondingly, $\tau = \beta/M$ is too large.

Discontinuities in classical distributions emerge, of course, in cases of discontinuous confining potentials only. These are more critical at the quantum limit and more different from the classical system, too. Thus, in our case in the horizontal harmonic potential the quantum limit is reached already with smaller Trotter numbers.

We should note that these distributions are essentially the same as those of Pi et al. [4] for the similar system. In their DFT study the number of electrons

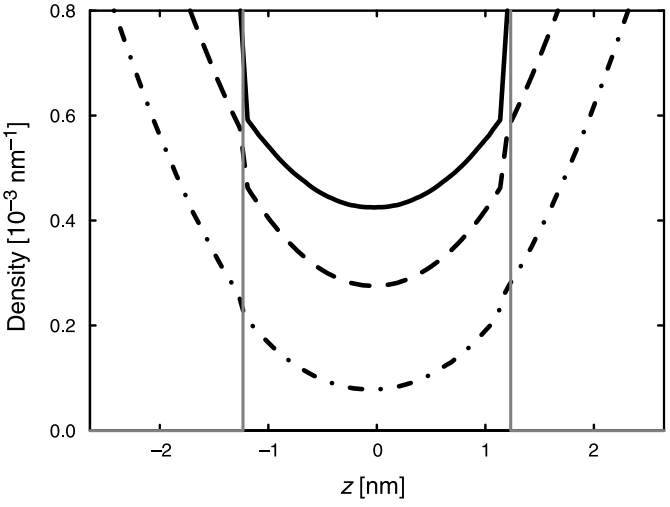

Fig. 3. Projected one-particle distribution functions in vertical (z) direction from simulations of a single electron with $(k_B\tau)^{-1} = (T \times M) = 3\,\mathrm{K} \times 2048 = 6144\,\mathrm{K}$, $10\,\mathrm{K} \times 2048 = 20480\,\mathrm{K}$, and $30\,\mathrm{K} \times 2048 = 61440\,\mathrm{K}$. The distributions are from 3 K (solid), 10 K (dashed), 30 (dash-dotted)

occupying the QDs was not found to essentially effect on the one-electron distributions, and our results for the two-electron case, below, support this general conclusion. However, there are small effects from electron-electron correlations, which we will analyze in what follows.

4.2 Two Interacting Electrons

Let us consider the system of two correlated electrons next and start by comparing the ''correlated'' one-electron distributions to the uncorrelated ones, i.e., to the single-electron distributions shown in Figs. 1 and 2. As the distributions are rather similar, we show the differences of those only in Figs. 4 and 5, respectively.

In both cases we see two expected main features. First, turning on electron-electron repulsion decreases the density where it is high, by shifting it to the less

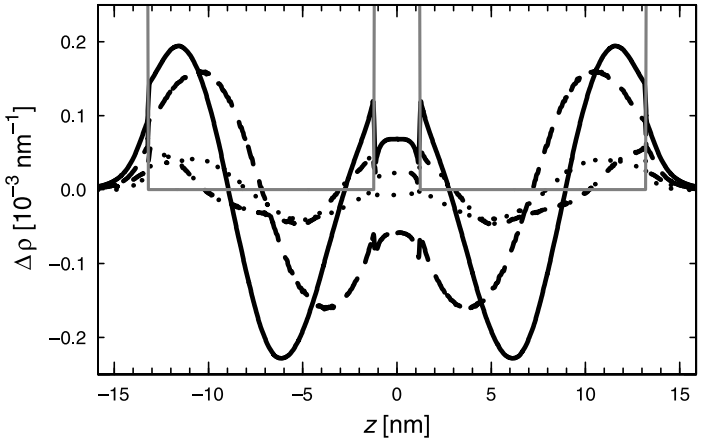

Fig. 4. Difference of the vertical (z) one-particle distribution function between the ''correlated'' two-electron and single-electron case. Thus, the two-electron distribution is a sum of the contributions given in Fig. 1 and this one. Note the different scaling of vertical axes in these figures. The notation for different temperatures is the same as in Fig. 1

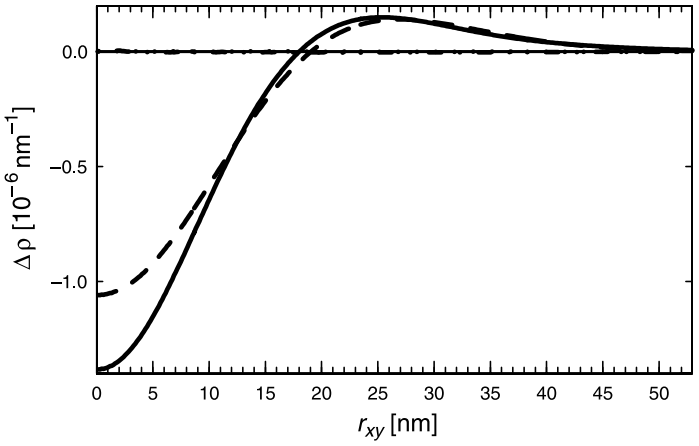

Fig. 5. Difference of the horizontal (*xy*) one-particle distribution function between the "correlated" two-electron and single-electron case. Again, the two-electron distribution is a sum of the contributions given in Fig. 2 and this one. The notation for different temperatures is the same as in Fig. 2

occupied regions of space. Secondly, the correlation effects are the larger the lower the temperature is.

In Fig. 4 the fine scaling zooms in the small discontinuities, which are visible at lower temperatures only, revealing that even larger Trotter numbers should be used to reach the quantum description limit more accurately. Fig. 5 shows that correlation effects are negligible in the horizontal distribution at the two highest temperatures, but essential at the two lower ones.

In Figs. 6 and 7 the two relevant projections of the pair correlation function in our case are shown, whereas Fig. 8 presents the conventional radial pair correlation function, good in characterizing isotropic systems. Clearly the vertical and radial functions reflect the same feature natural for a double QD: The electron correlation from repulsive interaction favors the case of one electron in each QD. This effect is stronger at the two lowest temperatures, as is seen in Fig. 6.

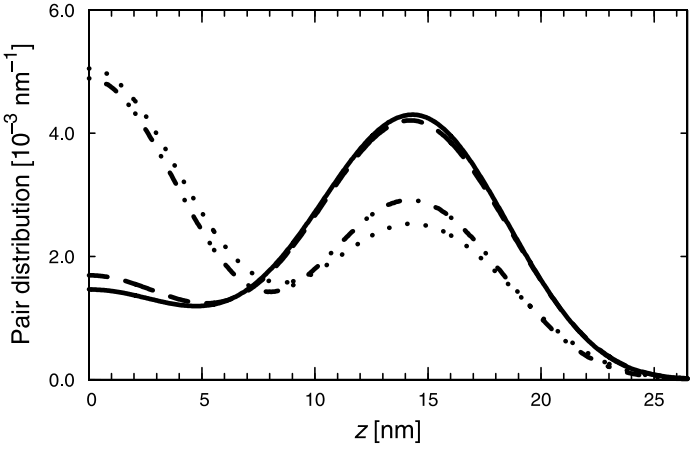

Fig. 6. Projected vertical (*z*) pair correlation function at various temperatures. The notation for different temperatures is the same as in Fig. 4

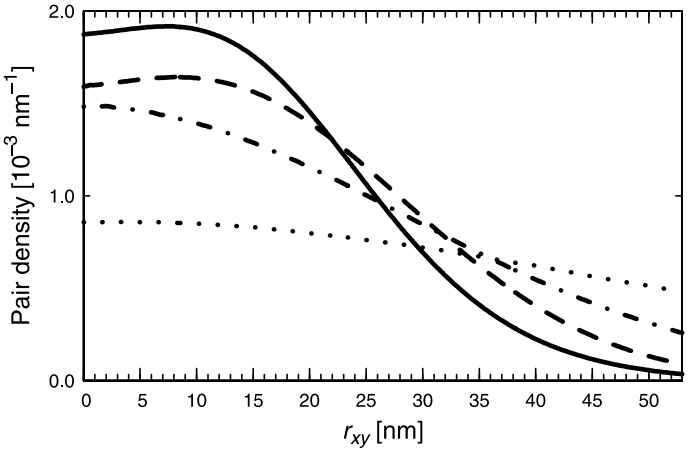

Fig. 7. Projected horizontal (xy) pair correlation function at various temperatures. The notation for different temperatures is the same as in Fig. 4

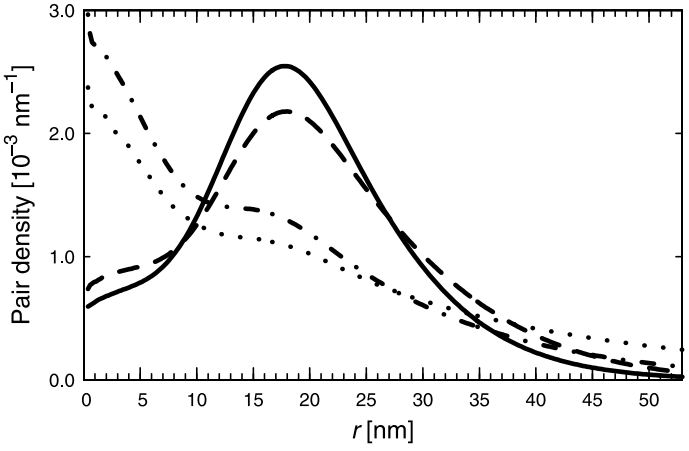

Fig. 8. (Radial) pair correlation function at various temperatures. The notation for different temperatures is the same as in Figs. 6 and 7

The dimensionality effect or separability of the three-dimensional system to the one- and two-dimensional subsystems can now be considered. The main question is: Does the small but finite vertical extension (z) have an essential effect on the electronic structure in the lateral (xy) plane [4, 6]? For the one-particle distribution the answer is obviously ''no'', because the one-particle distributions of the two-electron case and the single-electron case do not essentially differ and the latter is analytically separable to three dimensions. However, for the detailed two-electron distribution the answer is different as indicated by the low-temperature pair correlation functions. Clearly, at low temperatures where the electrons occupy the centre of the disc, see Figs. 7 and 6, the third dimension allows more freedom for this for both of the electrons simultaneously. However, the increase of temperature allows an occupation of the lateral space further away, which seems to cover the quantum and correlation effects.

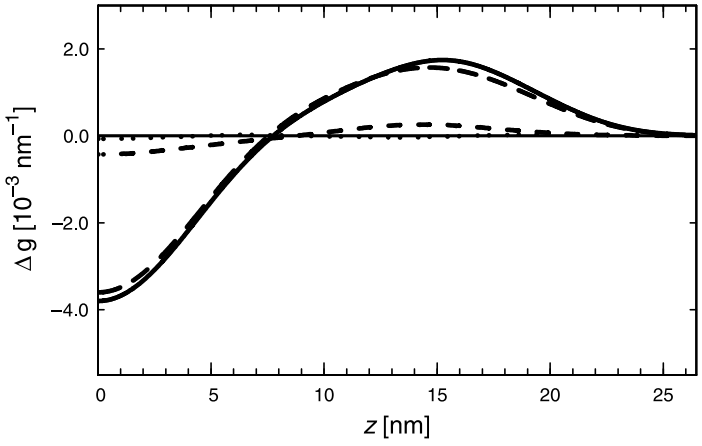

Fig. 9. Projected vertical (z) correlation hole at various temperatures

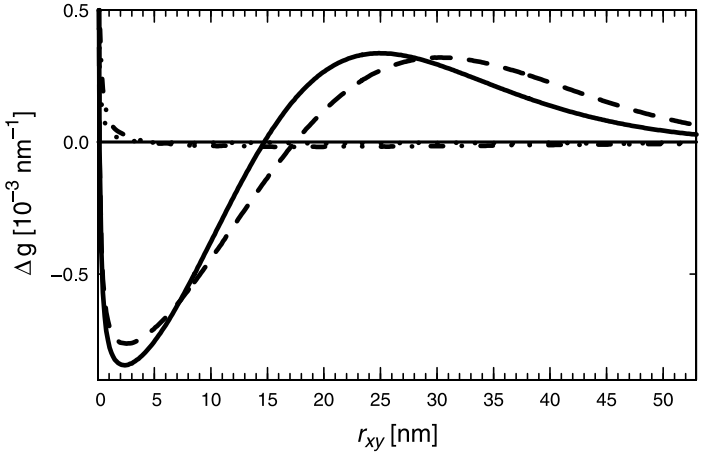

Fig. 10. Projected horizontal (xy) correlation hole at various temperatures

The same conclusions can be drawn from the correlation holes shown in Figs. 9 and 10. Here, the case is even more clear: At temperatures 100 and 300 K the presence of the second electron does not essentially effect on the dynamics of the first one. At lower temperatures 10 and 30 K, however, a more conventional correlation hole is seen, both vertically and laterally.

Table 1. Energetics of the two interacting electrons in the double quantum dot given per one electron. Uncertainty for the potential energy V_{pot} and mutual interaction energy V_{ee} are at least 5 and 0.5 meV, respectively

T [K]	V_{pot} [meV]	V_{ee} [meV]
3	15	2
10	15	2
30	10	2
100	15	2
300	30	1

Though we were able to reach a sufficient convergence for the distributions, regarding the energetics we are able to give rough estimates for some contributions only. These are presented in Table 1. The computational capacity gets a limitation, at lower temperatures in particular. Within the statistics, we are not able to find differences in the external potential energies of one of the interacting electrons and a single electron (or one of the two noninteracting ones). In both cases this potential-energy contribution grows from the zero-Kelvin quantum limit of about 15 meV to about 30 meV at 300 K, in fair agreement with the analytical single-electron case, where the total energies are 29 and 82 eV. The mutual Coulomb (repulsion) energy of the two electrons is about 1–2.5 meV, see Table 1. Surprisingly, only a small difference is found for two interacting electrons and two noninteracting ones, the latter one evaluated from the simulated noninteracting electron ''dynamics''. We are not able to obtain estimates for kinetic energies, the main reason being the discontinuous external potential function.

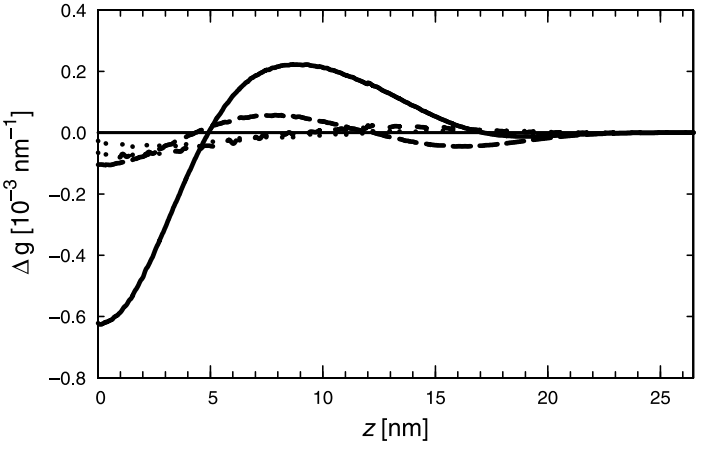

Fig. 11. Single QD case: Projected vertical (z) correlation hole

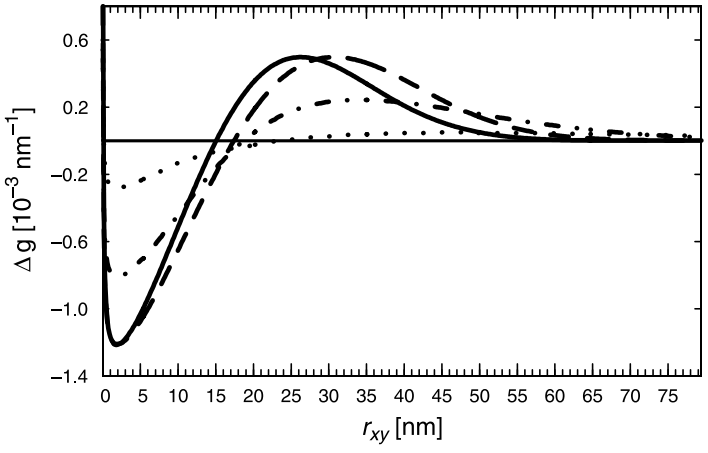

Fig. 12. Single QD case: Projected horizontal (xy) correlation hole

Finally, just for comparison, we consider the case of two electrons in *a single QD*, one of those coupled ones considered above. The projected correlation holes for this case are shown in Figs. 11 and 12 to be compared with Figs. 9 and 10. The stronger confinement in the vertical direction is seen directly in the vertical projection and indirectly in the horizontal projection. In the horizontal correlation this implies the temperature dependence even at higher temperatures. This is expected as there is less spatial freedom for electrons to occupy, unless thermally activated to higher quantum states.

5 Conclusions

We have shown that path-integral Monte Carlo (PIMC) simulations can be successfully carried out for one and two correlated electrons in a model quantum dot (QD). The case of ''spinless electrons'' of the two is considered only, and no magnetic field is applied in the studies reported here, either. We have considered disc-like, almost two-dimensional ''harmonic confinement QDs''. The main interest is in two QDs on top of each other and coupled through a narrow barrier, but a single one is considered for comparison.

The simulated one-particle distributions are very similar to those from the DFT calculations for the same system. With PIMC we find that the one-particle distributions for a single electron and for two electrons are almost identical in all cases independent of the temperature. Increase of temperature just broadens the distributions as expected, the effect being slightly smaller for correlated electrons than for the single one.

The Coulomb correlation of the two electrons is analyzed in terms of pair correlation functions and correlation holes. The perpendicular to the discs (vertical) and horizontal contributions are projected out from the fully 3D functions. This allows us to analyze the semiconductor dimensionality effect: Is the third dimension or the thickness of the almost two-dimensional disc-like QD essential for the horizontal distribution in the disc plane? The one-particle distributions are trivially separable to the vertical and horizontal contributions, but this turns out not to be the case for the two-particle distributions.

Generally, the correlations become more important at lower temperatures (10 and 30 K). At higher temperatures (100 and 300 K) the thermal broadening in the mixed quantum state description screens the correlation effect efficiently. For this reason, also the finite thickness of the QD disc is essential at the lower temperatures only, and also for the two-particle distribution only.

Evaluation of accurate energies takes more computational capacity than there is available today. This is true for the low-temperature quantum statistics in particular. Therefore, we are able to give rough estimates for some of the energy contributions only. We are able to predict that in case of our double QD structure the external potential energy is not strongly dependent on the temperature or correlation effects. Similarly, the mutual Coulomb energy seems to be constant throughout the various conditions of our system that we have considered.

We find that computational capacity becomes the limiting factor in simulations with increasing accuracy or with an increasing number of particles. In particular, this is true for fermion systems.

References

1. Kouwenhoven, L., Austing, D., Tarucha, S.: Rep. Prog. Phys. **64**, 701 (2001)
2. Reimann, S. M., Manninen, M.: Rev. Mod. Phys. **74**, 1283 (2002)
3. Harting, J.: PhD Thesis. University of Oldenburg 2001 (unpublished)
4. Pi, M., et al.: Phys. Rev. **B63**, 115316 (2001)
5. Leino, M., Rantala, T. T.: Physics Scripta **T114**, 44 (2004)
6. Rontani, M., et al.: Phys. Rev. **B59**, 10165 (1999)
7. Taut, M.: Phys. Rev. **A48**, 3561 (1993)
8. Dineykhan, M., Nazmitdinov, R.: Phys. Rev. **B55**, 13707 (1997)
9. Lin, J. T., Jiang, T. F.: Phys. Rev. **B64**, 195323 (2001)
10. Harju, A., Sverdlov, V., Nieminen, R.: Phys. Rev. **B59**, 5622 (1999)
11. Harju, A., et al.: Physica **B255**, 145 (1998)
12. Merkt, U., Huser, J., Wagner, M.: Phys. Rev. **B43**, 7320 (1991)
13. Ugajin, R., et al.: J. Appl. Phys. **76**, 1041 (1994)
14. Rontani, M., et al.: Solid State Commun. **119**, 309 (2001)
15. Burkard, G., Seelig, G., Loss, D.: Phys. Rev. **B62**, 2581 (2000)
16. Lee, E., et al.: Phys. Rev. **B57**, 12281 (1998)
17. Partoens, B., Peeters, F. M.: Phys. Rev. Lett. **84**, 4433 (2000)
18. Wensauer, A., et al.: Phys. Rev. **B62**, 2605 (2000)
19. Pi, M., et al.: Phys. Rev. Lett. **87**, 066801 (2001)
20. Imamura, H., Maksym, P. A., Aoki, H.: Phys. Rev. **B59**, 5817 (1999)
21. Tanaka, Y., Akera, H.: Phys. Rev. **B53**, 3901 (1996)
22. Rontani, M., et al.: Appl. Phys. Lett. **72**, 957 (1998)
23. Ezaki, T., Mori, N., Hamaguchi, C.: Phys. Rev. **B56**, 6428 (1997)
24. Lee, I.-H., et al.: Phys. Rev. **B57**, 9035 (1998)
25. Hirose, K., Wingreen, N. S.: Phys. Rev. **B59**, 4604 (1999)
26. Reusch, B., Häusler, W., Grabert, H.: Phys. Rev. **B63**, 113313 (2001)
27. Pederiva, F., Umrigar, C. J., Lipparini, E.: Phys. Rev. **B62**, 8120 (2000)
28. Häusler, W., et al.: Physica **B284**, 1772 (2000)
29. Mak, C., Egger, R., Weber-Gottschick, H.: Phys. Rev. Lett. **81**, 4533 (1998)
30. Egger, R., et al.: Phys. Rev. Lett. **82**, 3320 (1999)
31. Dikovsky, M. V., Mak, C. H.: Phys. Rev. **B63**, 235105 (2001)
32. Pollock, E. L., Ceperley, D. M.: Phys. Rev. **B30**, 2555 (1984)
33. Ceperley, D. M.: Rev. Mod. Phys. **67**, 279 (1995)
34. Feynman, R. P., Hibbs, A. R.: Quantum Mechanics and Path Integrals. New York: McGraw-Hill 1965
35. Feynman, R. P.: Statistical Mechanics. Reading, MA: Addison-Wesley 1972, 1988
36. Zong, F., Ceperley, D.: Phys. Rev. **E58**, 5123 (1998)
37. Harting, J., Mülken, O., Borrman, P.: Phys. Rev. **B62**, 10207 (2000)
38. Knoll, L., Marx, D.: Eur. Phys. J. **D10**, 353 (2000)
39. Gasiorowicz, S.: Quantum Physics. New York: Wiley 1996

Verleger: Springer-Verlag GmbH, Sachsenplatz 4–6, 1201 Wien, Austria. – Herausgeber: Prof. Dr. B. L. G. Bakker, Theoretical Physics Group, Department of Physics and Astronomy, Vrije Universiteit, De Boelelaan 1081, 1081 HV Amsterdam, The Netherlands. – Redaktion: De Boelelaan 1081, 1081 HV Amsterdam, The Netherlands. – Satz und Umbruch: Thomson Press (India) Ltd., Chennai. – Offsetdruck: Krips bv, Kaapweg 6, 7944 HV Meppel, The Netherlands. – Verlagsort: Wien. – Herstellungsort: Meppel. – Printed in The Netherlands.